Citation: Molecular Therapy—Nucleic Acids (2014) 3, e170; doi:10.1038/mtna.2014.28

www.nature.com/mtna

Genuine Immunomodulation With dSLIM

Kerstin Kapp[1], Christiane Kleuss[1], Matthias Schroff[1] and Burghardt Wittig[2]

Toll-like receptors are sensing modulators of the innate immune system. One member of this protein family, Toll-like receptor (TLR)-9, is increasingly being investigated as therapeutic target for infectious diseases and cancer. Double-Stem Loop ImmunoModulator (dSLIM) is a new TLR-9 agonist in clinical development for patients with metastatic colorectal carcinoma. Compared with other TLR-9 ligands developed as immunomodulators, dSLIM comprises single- and double-stranded DNA, is covalently closed, and consists of natural nucleotide components only. All investigated biologic effects of dSLIM are strongly dependent on CG motifs, and the relevant cellular activation profile of dSLIM is distinct to that of other TLR-9 agonists. Here we describe the structure and biologic profile of dSLIM: in isolated human peripheral blood mononuclear cells (PBMCs), dSLIM induced a unique pattern of cytokine secretion, activated within the PBMC pool particular cell subpopulations, and exhibited specific cytotoxicity on target cells. Using cellular isolation and depletion setups, the mechanism of immunoactivation by dSLIM was deduced to be dependent on, but not restricted to, TLR-9-bearing plasmacytoid dendritic cells. The dSLIM-promoted cellular stimulation directs systemic activation of the immune response as revealed in cancer patients. The observed cellular activation cascades are discussed in the context of cancer therapy.

Molecular Therapy—Nucleic Acids (2014) **3**, e170; doi:10.1038/mtna.2014.28; published online 24 June 2014
Subject Category: Nucleic acid chemistries Therapeutic proof-of-concept

Introduction

The mammalian immune system is composed of two major subdivisions, the innate or nonspecific immune system and the adaptive or specific immune system. While the innate immune response limits the early growth and spread of infectious organisms, only together with the subsequently mounted adaptive response most pathogens like viruses, bacteria, fungi, unicellular parasites can be finally warded off. Such infectious microorganisms are recognized via their pathogen-associated molecular patterns, such as lipoteichoic acid, lipopolysaccharides, or abundant nonmethylated CG motifs in DNA. The best characterized class of pathogen-associated molecular pattern sensors are the Toll-like receptors (TLRs).[1]

TLRs are classified according to the nature of their activating ligands, with TLR-9 recognizing bacterial DNA.[1] The presence of unmethylated cytosine-guanosine dinucleotides (CpG),[2] which are under-represented in nuclear DNA, allows mammalian cells to differentiate foreign bacterial DNA from self-DNA. Due to its bacterial endosymbiotic evolutionary history, self-mitochondrial DNA from energy-deficient cells with leaky mitochondria may bind and stimulate TLR-9. Thus, TLR-9 is the only dead-associated molecular pattern-detecting TLR in mammalian cells[3,4] and therefore an effective target for anticancer therapies.

TLR-9 is an intracellular protein, and is exclusively expressed in resting human immune cells by plasmacytoid dendritic cells (pDCs) and B lymphocytes (B cells).[5,6] Intracellular signaling triggered by TLR-9 activation results in recruitment of the myeloid differentiation primary response protein 88 (MyD88), that initiates a signaling cascade to activate (i) NFκB, leading to the production of proinflammatory cytokines and acquisition of antigen-presenting functions, and (ii) interferon (IFN) regulatory factor 7 (IRF7) activity leading to type I IFN production.[7,8] IFN-α released by pDCs[9] is a cytokine, which is central to linking the innate and adaptive immune response.[10,11] IFN-α activates monocytes, natural killer (NK) cell lytic activity, and IFN-γ secretion, and promotes the immunomodulatory functions of myeloid dendritic cells (mDCs) to initiate adaptive immune responses.[10] IFN-α induces B cells to differentiate and produce immunoglobulins.[10,12] Furthermore, upon TLR-9 activation, pDCs differentiate to direct T cell polarization by inducing upregulation of major histocompatibility complex class II and other T cell-activating molecules.[11]

Due to this double tracked activation of the immune system, TLR-9 agonists are promising therapeutics as vaccine adjuvants, anti-infectives, antiallergens, and anticancer tools.[7,13–15] In recent years, many TLR-9-binding ligands have been developed and classified according to structure and biologic profile into classes A, B, and C. Structurally, all those TLR-9-binding ligands are composed of short linear DNA molecules with phosphothioester bonds in the DNA backbone (phosphorothioate oligonucleotide), differing in their base sequence, extent of phosphorothioate oligonucleotide modification, and aggregation potential. Class A agents strongly induce IFN-α secretion from pDCs, but only moderate pDC maturation and poor activation of B cells.[16,17] In contrast, class B agents, such as ODN2006 (also known as CPG7909 or PF-3512676), induce poor IFN-α secretion from pDCs, but are strong activators of pDC maturation and B cells.[17,18] Class C agents, such as M362, have immunomodulatory properties intermediate between class A and B ODN, induce strong IFN-α secretion and high expression of costimulatory molecules on pDCs.[19,20]

dSLIM (double-Stem Loop ImmunoModulator; MGN1703) is a covalently closed DNA molecule, does not contain any

The first two authors contributed equally to this work.
[1]Mologen AG, Berlin, Germany; [2]Foundation Institute Molecular Biology and Bioinformatics, Freie Universitaet Berlin, Berlin, Germany. Correspondence: Christiane Kleuss, Mologen AG, Fabeckstraße 30, D-14195 Berlin, Germany. E-mail: kleuss@mologen.com
Keywords: cancer immunotherapy; immune cell activation; immune modulation; immuno-oncology; innate immunity; MGN1703; pDC
Received 4 February 2014; accepted 29 April 2014; published online 24 June 2014. doi:10.1038/mtna.2014.28

unnatural modification, and has a dumbbell-shaped structure. This immunomodulatory agent is constituted by two single-stranded loops of 30 nucleotides each. The two loops are spanned and spaced by a double-stranded stem of 28 base pairs. Both loops comprise three effective nonmethylated CG motifs conferring exact point symmetry to dSLIM. dSLIM was designed by B.W. and is proprietary of Mologen AG. The rational design was based on a stretch of immunostimulatory sequences present in the ampR gene found in bacteria[21] that B.W. embedded in a flexible and easily accessible conformation: the single-stranded DNA loops. Both loops were connected by a double-stranded DNA stem serving several purposes: (i) conferring stability against exonuclease activity by avoiding free 3′-OH groups in dSLIM, (ii) avoiding artificial DNA-protecting groups like phosphorothioates that were realized to elicit unwanted effects in mammalian organisms,[22,23] (iii) spacing both sets of immunostimulatory sequences of the loops in a flexible and effective distance, (iv) clustering sets of immunostimulatory sequences of the loops in an effective, known, and controllable ratio.

The unique structure of dSLIM results in an immunoreactive cellular activation profile that differs from that triggered

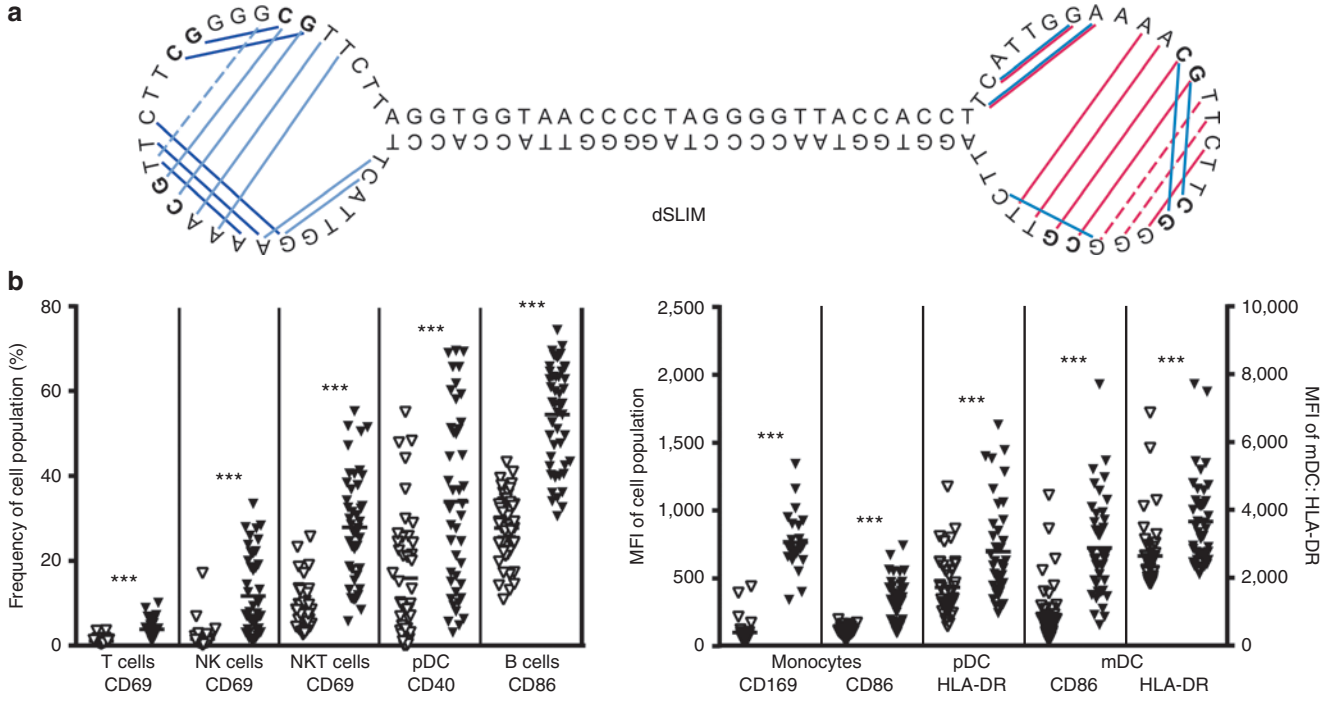

Figure 1 Structure of double-Stem Loop ImmunoModulator (dSLIM) and cellular activation of human peripheral blood mononuclear cells (PBMCs) by dSLIM. (**a**) Sequence and conformation of dSLIM under isotonic conditions. Potential base pairings in the loop structures were predicted for 4, 37, and 80 °C by bioinformatical tools, and are indicated by lines connecting pairing bases. Blue lines indicate base pairings at ~4 °C, red lines indicate base pairing at 37 °C, different blue or red tones indicate mutually exclusive pairing scenarios, and dashed lines indicate unusual base pairing of G:T near relatively strong intraloop hybrid structures. For clarity, different interaction scenarios are shown in each loop although each loop may adopt all scenarios shown in either loop depending on temperature. (**b**) Cellular activation of human PBMCs. PBMCs were treated without (open triangles) or with dSLIM (filled triangles) at a final concentration of 3 µmol/l for 48 hours. Cells were stained with antibodies against lineage and the indicated activation markers. Frequencies or mean fluorescent intensity of activation markers within the cell populations are shown (means are shown; CD86 of monocytes, $n = 50$; CD86 of B cells, $n = 48$; CD86 of mDCs; CD69 of T cells, NK cells, and NKT cells, $n = 44$; HLA-DR of mDCs and CD40 of pDCs, $n = 43$; HLA-DR of pDCs, $n = 41$; CD169 of monocytes, $n = 39$; ***$P < 0.001$; paired *t*-test).

Table 1 Induction of natural killer cell (NK cell)–mediated cytotoxicity in PBMCs

	Effector: target 20:1 ($n = 13$)			Effector: target 10:1 ($n = 13$)			Effector: target 5:1 ($n = 13$)		
Specific cytotoxicity[d] (%)	PBMC[a]	PBMC + dSLIM[b]	PBMC + IL-2[c]	PBMC[a]	PBMC + dSLIM[b]	PBMC + IL-2[c]	PBMC[a]	PBMC + dSLIM[b]	PBMC + IL-2[c]
Mean[e]	28.69	46.66*,[f]	72.12*,[f]	15.58	32.81*,[f]	57.56*,[f]	7.34	18.16*,[f]	40.31*,[f]
SEM[e]	3.74	4.46	4.02	2.66	4.21	4.60	1.23	2.85	5.21

AAD, amino-actinomycin D; dSLIM, double-Stem Loop ImmunoModulator; PBMC, peripheral blood mononuclear cell; SEM, standard error of the mean. [a]Negative control: PBMCs were incubated in complete medium. [b]PBMCs were incubated in complete medium supplemented with dSLIM to a final concentration of 3 µmol/l.[c]Positive control: PBMCs were incubated in complete medium supplemented with recombinant IL-2 to a final concentration of 2,000 U/ml. [d]PBMCs were incubated for 48 hours. Thereafter, PBMCs were cocultured for 4 hours with the stated fraction of DiI-labeled Jurkat cells as targets. After staining with 7-AAD, specific cytotoxicity was estimated based on the frequencies of 7-AAD-positive target cells. [e]Means and SEM of the specific cytotoxicity are calculated as described in Materials and Methods; data from 13 independent experiments are shown. [f]The differences in the calculated specific cytotoxicities of PBMCs between dSLIM-treated PBMCs and negative control are significant.*$P < 0.001$; repeated measures analysis of variance; Dunnett's multiple comparison test.

by linear, single-stranded, phosphorothioate oligonucleotide-modified TLR-9 agonists. Here we describe the effect of dSLIM on the human immune response, in particular cytokine secretion and activation of immune cells and their subpopulations via pDC activation. These events trigger both the innate and the adaptive arm of the immune response that together are mandatory for the effective elimination of malignant cells from the body.

Results

Structure and physic parameters of dSLIM

dSLIM is a small DNA molecule built from 116 nucleotides, linked into a circular, nonbranched structure by natural phosphodiester bonds. The internal stretches of reverse complementary DNA sequences result in the formation of a covalently closed dumbbell-shaped molecule, comprising of two single-stranded loops connected by a double-stranded stem (**Figure 1a**). All loop bases, in particular the three CG motifs, are present in a dimer constellation; the bending capability of the bridging stem results in an adjustable space between the loop bases. The stem was identified to be a highly rigid double-stranded DNA, with a melting temperature of 83 °C at the experimental salt concentration (**Supplementary Data**, **Supplementary Figure S1**). Due to the closed circular structure, dSLIM is protected against exonuclease activity. As depicted in the **Supplementary Figure S2**, the conformational guard apparently protected better than phosphorothioate modifications at the backbone: the latter just retarded, but did not impede degradation.

Biologic effects of dSLIM

Cellular activation. Within the peripheral blood mononuclear cell (PBMC) pool, activation of relevant immune cells upon dSLIM exposure was evident and significant ($P < 0.001$; **Figure 1b**): CD40 was upregulated on pDCs, as well as HLA-DR (major histocompatibility complex class II). Also, more HLA-DR per cell was expressed by mDCs that concomitantly boosted up CD86 assembly at their plasma membrane. B cells were activated as shown by additional B cells expressing CD86. Monocyte activation was indicated by upregulation of CD86 and CD169 expression.

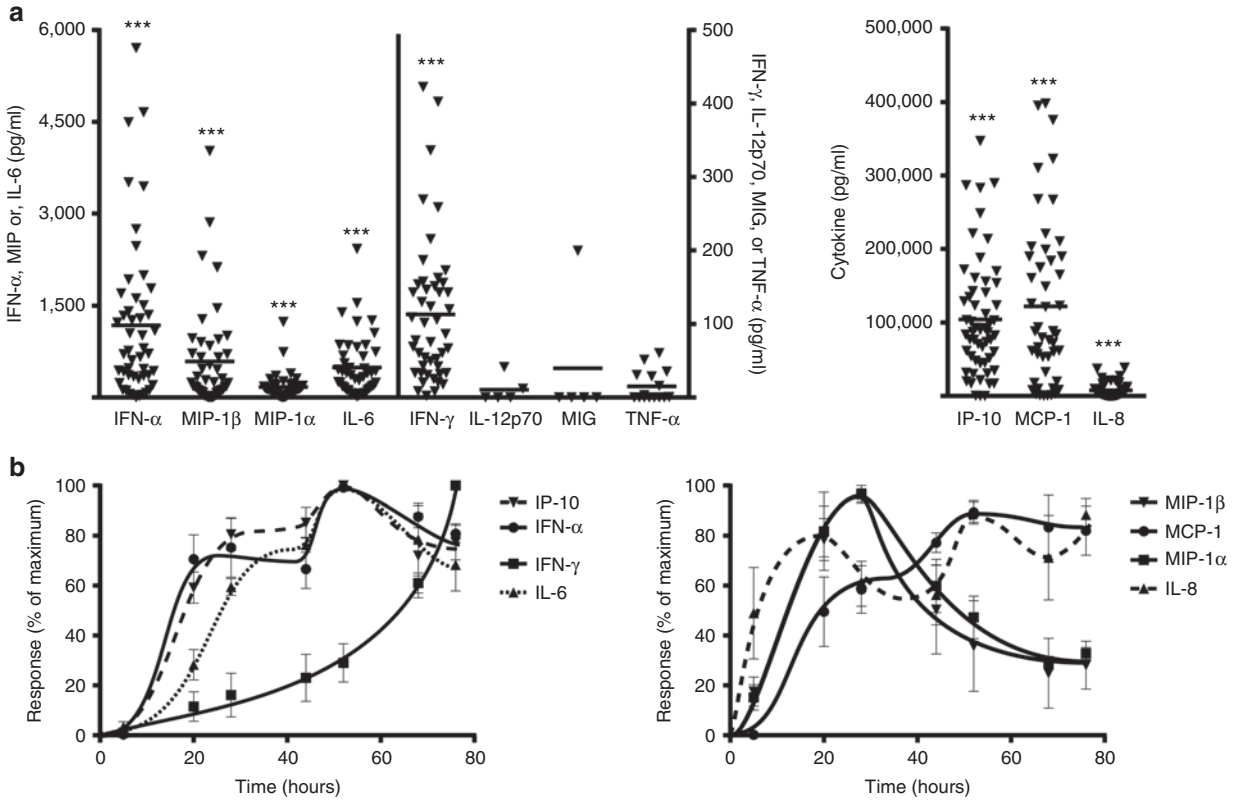

Figure 2 Cytokine secretion by peripheral blood mononuclear cells (PBMCs). PBMCs were treated with double-Stem Loop ImmunoModulator (dSLIM) at a final concentration of 3 µmol/l. Cytokine levels in the supernatants were determined by a bead-based multiplex immunoassay or enzyme-linked immunosorbent assay. (**a**) Secreted cytokines from PBMCs treated with dSLIM for 48 hours. Results of individual experiments are shown as analyzed cytokine concentrations corrected for basal concentrations obtained from cells incubated under identical conditions but in the absence of dSLIM (medium control; means are shown; IP-10, $n = 56$; IL-8, $n = 51$; IFN-α, $n = 49$; MCP-1, $n = 48$; IFN-γ, $n = 47$; MIP-1α, MIP-1β, and IL-6, $n = 45$; TNF-α, $n = 15$; IL-12p70 and monokine induced by γ-IFN, $n = 5$; differences between dSLIM-treated PBMCs and medium control are significant for the indicated cytokines; ***$P < 0.001$; paired *t*-test). (**b**) Time course of cytokine secretion. After the indicated time points, cell culture supernatants were withdrawn and analyzed. The estimated cytokine concentrations were normalized to the maximal concentration for each cytokine in the individual experiment (IFN-γ: 239–396 pg/ml; MIPβ: 641–9,223 pg/ml; MIP-1α: 273–3,300 pg/ml; IL-6: 421–2,486 pg/ml; IFN-α: 584–2,020 pg/ml; MCP-1: 64,440–468,803 pg/ml; IL-8: 814–76,117 pg/ml; IP-10: 91,068–305,908 pg/ml). Means and SEM from four individual experiments are shown IP-10, dashed line, triangle down; IFN-α, circle; IFN-γ, squares; IL-6, dotted line, triangle up. IL-8, dashed line, triangle up; MCP-1, circle; MIP-1-α, squares; MIP-1-β, triangle down.

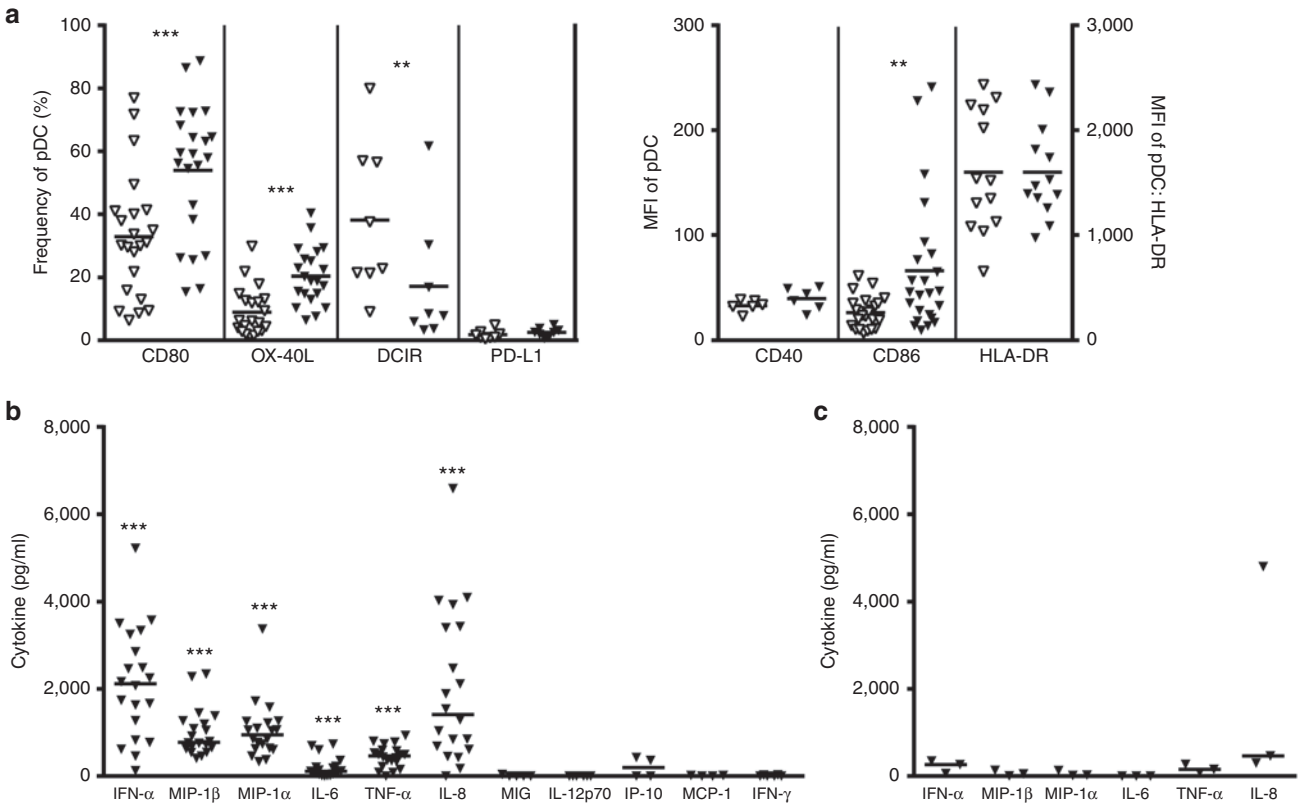

Figure 3 Activation of plasmacytoid dendritic cells (pDCs). Isolated pDCs were treated with double-Stem Loop ImmunoModulator (dSLIM) (**a**,**b**) or a non-CG dSLIM (**c**) for 48 hours at a final concentration of 3 µmol/l in the presence of IL-3. (**a**) Expression of activation markers. Frequencies or mean fluorescent intensity of the analyzed activation markers are shown (open triangles, pDCs incubated in medium in the absence of dSLIM; filled triangles, pDCs incubated in medium in the presence of dSLIM (means are shown; CD86, $n = 24$; CD80, $n = 22$; OX-40L, $n = 21$; HLA-DR, $n = 13$; dendritic cell immunoreceptor (DCIR) and PD-L1, $n = 8$; CD40, $n = 6$; $^{**}P < 0.01$; $^{***}P < 0.001$; paired *t*-test). (**b**) Cytokines secreted from pDCs after incubation with dSLIM. Cytokine levels in the supernatants of pDCs were determined by a bead-based multiplex immunoassay. Cytokine levels of cells were corrected for background levels obtained after incubation of cells in medium without dSLIM. Differences between dSLIM-treated pDCs and medium were significant for the indicated cytokines (means are shown; $n = 20$ for most cytokines except: monokine induced by γ-IFN (MIG), $n = 5$; IL-12p70 and IFN-γ, $n = 6$; IP-10 and MCP-1, $n = 4$; $^{***}P < 0.001$; paired *t*-test). (**c**) Cytokines secreted from pDCs after incubation with non-CG dSLIM. Cytokine levels in the supernatants of non-CG dSLIM-treated pDCs were determined as described for panel B (means are shown; $n = 3$).

NK, natural killer T cells NKT, and T cells were induced by dSLIM to express the activation marker CD69. NK cell activation was also monitored by the elevated cytotoxicity against target cells: PBMCs treated with dSLIM showed a concentration-related NK-cell–dependent cytotoxicity against Jurkat cells (**Table 1**). All cellular activations were dependent on dSLIM CG-motifs and were not elicited by exposure of PBMCs to a molecule with T exchanged for C in all 6 CG motifs (**Supplementary Figure S3**).

Cytokine secretion from PBMCs. Secretion of IFN-α, macrophage inflammatory protein (MIP)-1α, MIP-1β, IL-6, IFN-γ, IFN-γ-induced protein 10 (IP-10), monocyte chemotactic protein (MCP)-1, and IL-8 from PBMCs was significantly increased by dSLIM. No alterations in secretion of IL-12p70, monokine induced by γ-IFN (MIG) and tumor necrosis factor (TNF)-α were detected (**Figure 2a**). Also, secretion of cytokines was dependent on the presence of CG-motifs in dSLIM (**Supplementary Figure S4**).

Assessment of cytokine secretion by PBMCs over 80 hours revealed a release of most cytokines during the first 48 hours of exposure to dSLIM (**Figure 2b**). The low IFN-α levels measured in PBMCs (compare IFN-α concentrations measured in the supernatant from isolated pDCs, see "cellular targets") were most probably caused by cellular consumption of secreted IFN-α before measurement. A slow time course was charted for IFN-γ release, which secretion increased slowly and progressively during the 80 hours period and did not reach plateau level. MIP-1α and MIP-1β concentrations showed the fastest time course of the cytokines monitored, and peaked after ~30 hours. After this time, levels declined presumably due to consumption and/or degradation.

Cellular targets of dSLIM

TLR-9-positive cells: pDCs. In isolated pDCs, dSLIM was associated with significant upregulation of the costimulatory molecules CD80, OX-40L, and CD86 (**Figure 3a**), while repressive molecules were not positively modulated by dSLIM: the immunosuppressive protein programmed cell death receptor 1 (PD-L1) ligand was expressed only on a minority of pDCs and was not upregulated upon dSLIM incubation; the inhibitory dendritic cell immunoreceptor (DCIR) was significantly downregulated after exposure to dSLIM.

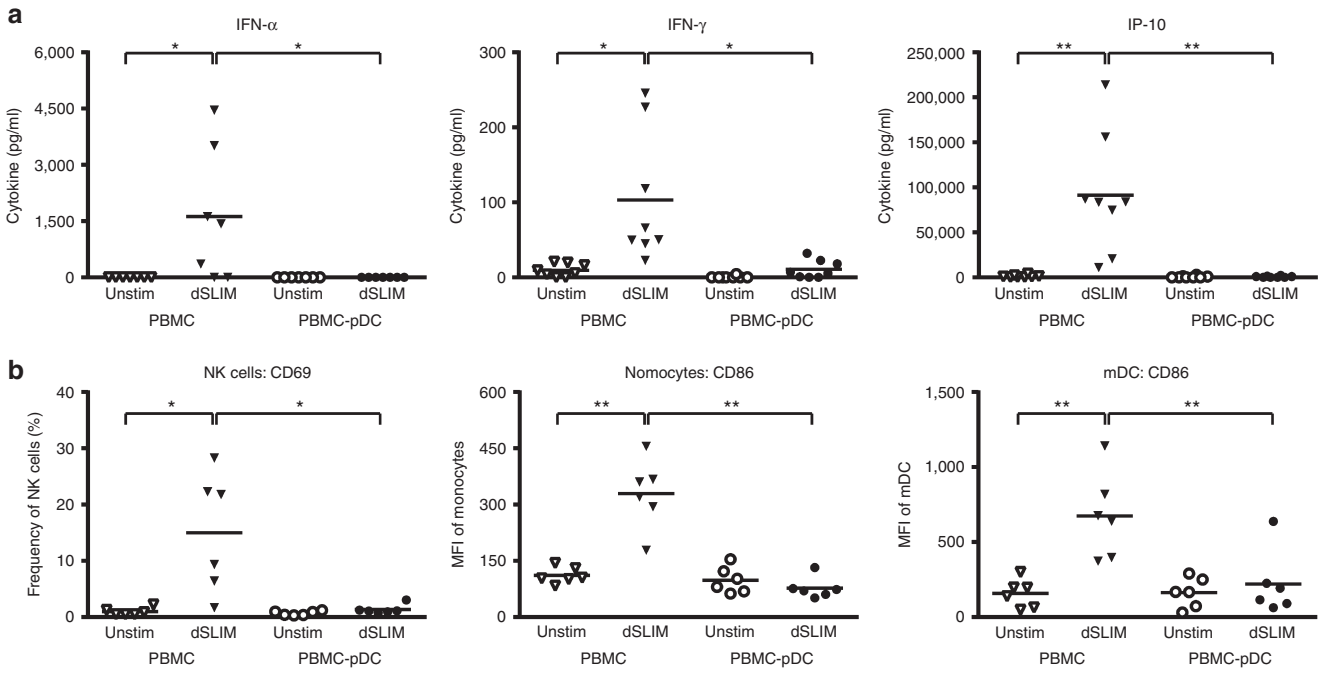

Figure 4 Plasmacytoid dendritic cell (pDC)-dependent immune response in peripheral blood mononuclear cells (PBMCs). PBMCs (triangle down) and pDC-depleted PBMCs (circle) were treated with double-Stem Loop ImmunoModulator (dSLIM) (filled symbols) at a final concentration of 3 µmol/l for 48 hours or with medium alone (open symbols). Differences between dSLIM-treated PBMCs and medium alone-treated PBMCs, as well as dSLIM-treated PBMCs and dSLIM-treated pDC-depleted PBMCs were statistically analyzed. (**a**) Cytokines in the supernatant. Cytokine levels in the supernatants were determined by a bead-based multiplex immunoassay or enzyme-linked immunosorbent assay (means are shown; IFN-α, $n = 7$; IFN-γ and IP-10, $n = 8$, repeated measures analysis of variance (ANOVA); Fisher's least significant difference (LSD) test). (**b**) Activation markers. Cells were stained with antibodies against lineage and the indicated activation markers. Frequencies or mean fluorescent intensity of the indicated activation markers within the cell populations are shown (means are shown; $n = 6$; $^*P < 0.05$; $^{**}P < 0.01$; repeated measures ANOVA; Fisher's LSD test).

The pattern of cytokine secretion from pDCs was particular to dSLIM and was strongly dependent on the presence of CG motifs in dSLIM: induction of IFN-α, MIP-1β, MIP-1α, IL-6, TNF-α, and IL-8 secretion was significantly increased in pDCs cultured in the presence of dSLIM compared with medium alone (**Figure 3b**). However, these cytokines were barely induced in pDCs cultured with a dSLIM derivative that had the six CpGs in the loop CG motifs replaced by TpG each (non-CG dSLIM; **Figure 3c**).

From PBMCs devoid of pDCs, no IFN-α release was detected after incubation with dSLIM (**Figure 4a**). Consequently, in the absence of pDCs as main producer of IFN-α in PBMCs, also activation of the main cellular targets responding to IFN-α (NK cells, monocytes, and mDCs) was abrogated in pDC-depleted PBMC (**Figure 4b**). Further, neither IFN-γ nor IP-10 secretion was monitored in pDC-depleted PBMCs (**Figure 4a**). Given that IFN-γ and IP-10 were not found to be secreted by isolated pDCs, it is likely that the production of these cytokines was due to an indirect effect of dSLIM on TLR-9-negative cells within the PBMC pool.

TLR-9-positive cells: B cells. dSLIM activated isolated human B cells but less pronounced than pDCs. dSLIM exposure of isolated B cells resulted in an increased number of cells expressing CD80 and CD86, as well as CD40. However, no change in HLA-DR expression was observed (**Figure 5a**). Increased secretion of MIP-1α, IL-6, TNF-α, and IL-8 was observed in B cells cultured with dSLIM compared with medium alone (**Figure 5b**). Secretion of MIP-1-β and MCP-1 was also induced, but levels did not differ significantly from the dSLIM-free culture conditions. The most relevant cytokines secreted by PBMCs upon dSLIM incubation, IFN-α, IP-10, and IFN-γ, were not detected in the supernatants of isolated B cells. B cell-depleted PBMCs cultured with dSLIM showed reduced release of IFN-γ and IP-10, and resulted in almost complete inhibition of MCP-1 secretion compared with nondepleted PBMCs cultured in the presence of dSLIM (**Figure 5c**). In contrast to the unresponsiveness of TLR-9-negative cells in pDC-depleted PBMCs, removal of B cells from PBMCs significantly reduced, but did not blunt dSLIM-associated cytokine secretion (IFN-γ and IP-10) and cellular activation of NK cells, mDCs, and monocytes (data not shown).

TLR-9-negative cells: monocytes. Although monocytes are devoid of TLR-9, they are stimulated upon dSLIM exposure in the context of PBMC culturing. Intracellular flow cytometry revealed monocytes as the main producer of IP-10 within PBMCs after dSLIM exposure (**Supplementary Figure S5**). Apparently, monocytes were also an important amplificator for IFN-α release probably via a feed forward mechanism as dSLIM-triggered IFN-α secretion significantly dropped after monocyte depletion from PBMC; IFN-γ release from PBMC was unaffected by the absence or presence of monocytes.

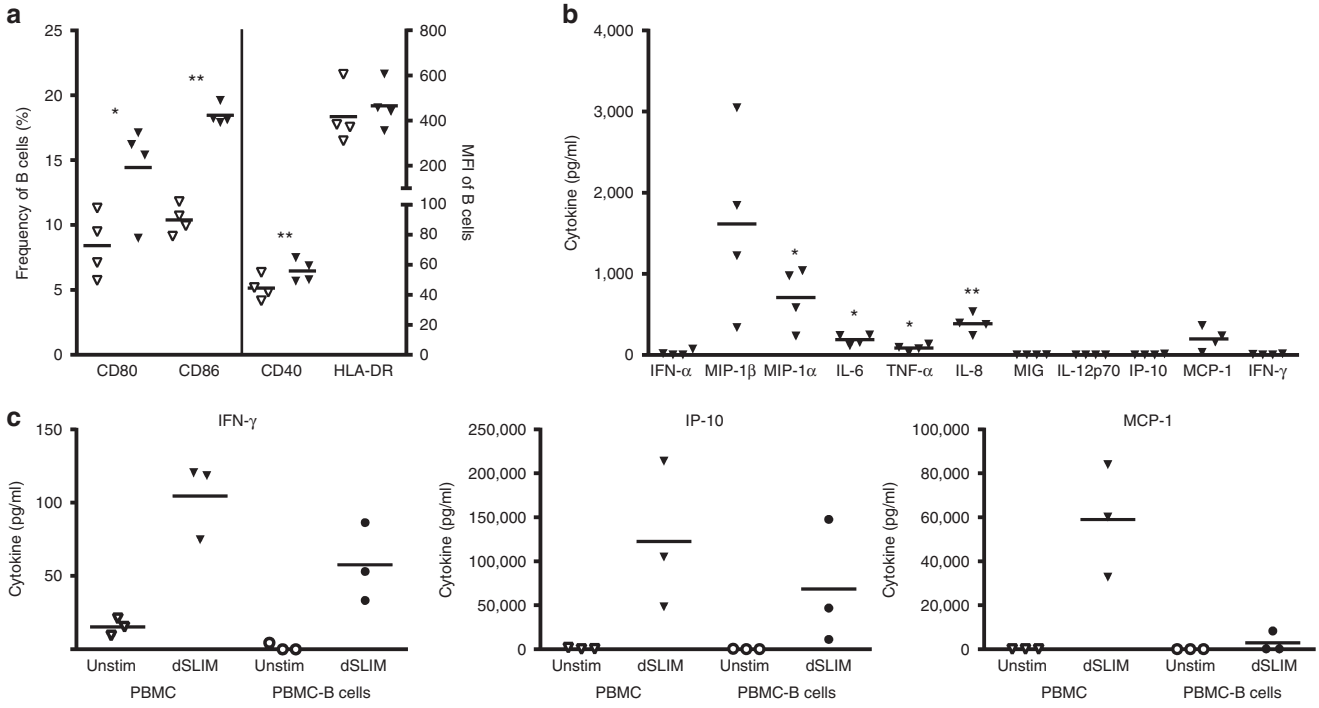

Figure 5 Activation of B cells and B cell-dependent cytokine response in the peripheral blood mononuclear cell (PBMC) pool. Cells were treated for 48 hours with double-Stem Loop ImmunoModulator (dSLIM) at a final concentration of 3 µmol/l (filled symbols) or in the absence of dSLIM (medium control, open symbols). (**a,b**) Activation of isolated B cells with dSLIM. (**a**) Expression of activation markers. Frequencies or mean fluorescent intensity of the analyzed activation markers are shown (means are shown; $n = 4$; $^*P < 0.05$; $^{**}P < 0.01$; paired *t*-test). (**b**) Cytokine secretion. Cytokine levels in the supernatants of dSLIM-treated isolated B cells were determined by a bead-based multiplex immunoassay. Cytokine levels of medium control were subtracted from the correspondent levels obtained after dSLIM treatment. Differences between dSLIM-treated B cells and medium control were significant for the indicated cytokines (means are shown; $n = 4$; $^*P < 0.05$; $^{**}P < 0.01$; paired *t*-test). (**c**) Role of B cells for the cytokine secretion from PBMCs. PBMCs and B cell-depleted PBMCs were treated with dSLIM and cytokine levels in the supernatants were determined by enzyme-linked immunosorbent assay (means are shown; $n = 3$).

Pharmacodynamics of dSLIM

Activation of an NFκB reporter cell line, ELAM41, by dSLIM was dose dependent and plateaued above 3 µmol/l (**Figure 6a**). In ELAM41 cells, dSLIM activated enhanced green fluorescent protein (eGFP)-mediated fluorescence (a measure of TLR-9 activation) with an EC_{50} of ≈100 nmol/l. A dSLIM derivative with all CpGs in the loop CG motifs replaced by TpG did not induce eGFP expression. A concentration-dependent saturation (0.2–20 µmol/l dSLIM) was evident in PBMCs where dSLIM activity was measured as release of either IP-10, IFN-α, or IFN-γ (**Figure 6b**). A similar relationship was observed in TLR-9-negative NK cells in the context of PBMCs (**Figure 6c**). In TLR-9-positive cells, *i.e.*, B cells and pDCs, induction of the activation marker CD86 was also strongly concentration-dependent, but did not saturate up to 20 µmol/l dSLIM (**Figure 6d**).

Comparison with immunomodulatory CpG ODNs

In addition to its sequence, base composition and conformation, all essentially distinct to class A, B, and C ODN, dSLIM also differs in terms of its immunomodulatory effects, both in potency and mechanism: the potency of dSLIM (EC_{50}: 0.1 µmol/l) in TLR-9-positive ELAM41 cells was much higher than that developed by either class of CpG ODN (EC_{50} of class A ODN ODN2216: 1.5 µmol/l, EC_{50} of class B ODN ODN2006: 0.4 µmol/l, and EC_{50} of class C ODN M362: 0.8 µmol/l; **Figure 7a**).

The stimulatory effect of TLR-9 agonists can be inhibited by chloroquine, a lysosomotropic agent that prevents endosomal acidification.[24] ODN2216, ODN2006, and M362, as well as dSLIM activation of ELAM41 cells were inhibited in a concentration-dependent manner by chloroquine (**Figure 7b**). Interestingly, the observed IC_{50} values for chloroquine on ELAM41 cells that had been half maximally stimulated by TLR-9 agonists of the different classes, differed but did not reflect the EC_{50} values of those TLR-9 agonists. While dSLIM needed the lowest amount of all investigated TLR-9 agonists to half maximally stimulate the TLR-9 pathway, it required the highest chloroquine concentrations in order to be inhibited at the internalization step. On the other hand, ODN2216 was half maximally effective at the highest concentration (1.5 µmol/l) of all TLR-9 agonists investigated; the concentration of chloroquine required to blunt this low potent ODN2216 activation was almost as high as that required to blunt ELAM41 cell stimulation by the highly potent dSLIM while the medium potent ODN2006 activations and M362 activations were very sensitive for chloroquine inhibition.

In the complex system of PBMC activation, the stimulatory profiles of ODN2216 and ODN2006 varied, and were also different to the dSLIM footprint. While secretion of IFN-γ from PBMCs was observed following incubation with dSLIM, ODN2006, and ODN2216, secretion of IFN-α and IP-10 was

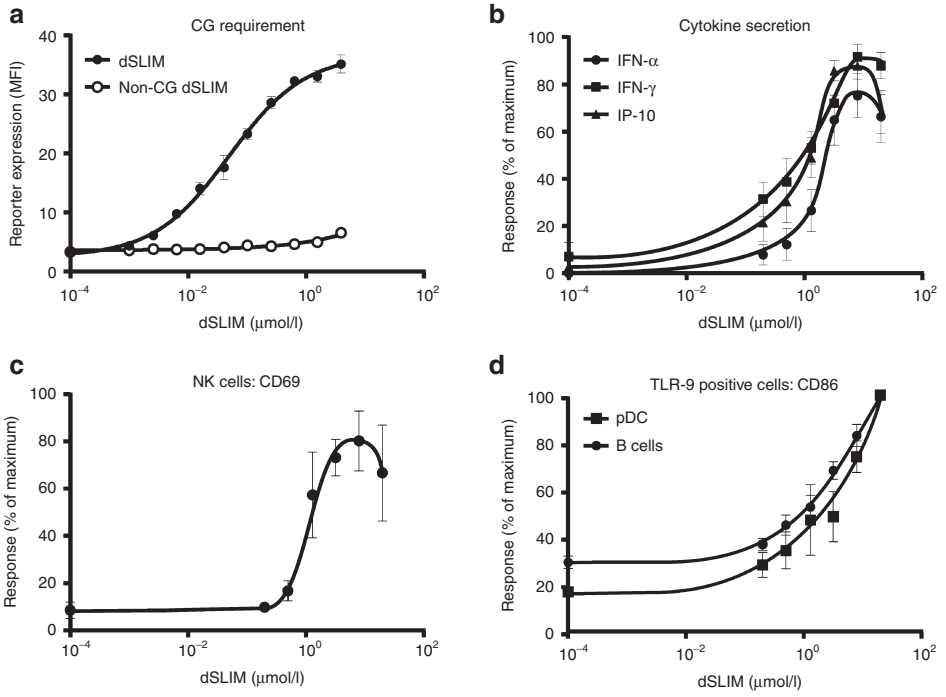

Figure 6 Concentration-dependent activation by double-Stem Loop ImmunoModulator (dSLIM). Cells were treated with dSLIM at the indicated final concentrations ranging from 0.2 to 20 μmol/l. (**a**) Toll-like receptor (TLR)-9 reporter cell. ELAM41 cells were treated with dSLIM (filled circle) or non-CG dSLIM (open circle) for 7 hours. Means and standard error of the mean (SEM) from six (dSLIM) and three (non-CG dSLIM) individual experiments are shown. (**b**) Cytokines secreted from peripheral blood mononuclear cells (PBMCs) incubated with dSLIM for 48 hours. Cytokine levels in the supernatants were determined by a bead-based multiplex immunoassay or enzyme-linked immunosorbent assay. For each individual experiment and cytokine, the analyzed concentration was normalized to the maximal concentration secreted (IFN-γ: 105–715 pg/ml; IFN-α: 45–1,782 pg/ml; IP-10: 19,276–290,295 pg/ml). Means and SEM resulting from the stated numbers of individual experiments are shown (IFN-α, circle, $n = 11$; IFN-γ, square, $n = 5$; IP-10, triangle, $n = 12$). (**c,d**) Expression of activation markers within selected cell populations of human PBMCs. Cells were stained with antibodies against lineage and the indicated activation markers. The measured mean fluorescent intensity (CD86 of plasmacytoid dendritic cells (pDCs) and B cells) or frequency (CD69 of NK cells) of activation markers within the analyzed cell populations were normalized to the maximal values obtained for each analyte in the individual experiment (CD69 of NK cells 2.6–9.9%; CD86 of B cells mean fluorescent intensity 15.5–26.5; CD86 of pDCs mean fluorescent intensity 46.7–572). Means and SEM resulting from the stated number of individual experiments are shown (CD69 of NK cells n = 4 in **c**, CD86 of B cells, $n = 5$, circles; CD86 of pDCs, $n = 4$, squares in **d**).

only observed following incubation with dSLIM and ODN2216 (**Figure 7c**). While ODN2216 was a better IFN-α inducer, PBMCs released marginally more IP-10 upon dSLIM incubation than in the presence of ODN2216; ODN2006 induced neither IFN-α nor IP-10 secretion at the common agonist concentrations (3 μmol/l). However, ODN2006 could induce some IFN-γ, low IFN-α, and marginal IP-10 secretion at minor concentrations applied (**Supplementary Figure S6**). Activation of immune cells indicated by the expression level of surface markers also differed according to the type of TLR-9 agonist. ODN2006 was a poor activator of monocytes and NK cells, while ODN2216 and dSLIM activated monocytes to almost the same extent; however, ODN2216 activated more NK cells than was observed with equimolar dSLIM concentrations (**Figure 7d**). The 3 μmol/l concentrations of all TLR-9 agonists investigated were above the individual EC_{50} values for ELAM41 cells, and were able to provoke maximal responses across all measured parameters in PBMCs; therefore, the observed differences in efficacy reflect TLR-9 agonist-specific features rather than insufficient occupancy of the TLR-9 receptor.

Discussion

dSLIM is an immunomodulatory, noncoding DNA molecule with a base sequence that accounts for one-twentieth a microbial gene sequence.[21] Although dSLIM is synthesized *de novo* on a solid-phase synthesizer, it contains only natural components connected by phosphodiester bonds comprised in genuine DNA. Due to the presence of clustered unmethylated CpGs in the single-stranded loops, dSLIM activates a broad set of immune cells either directly or via activation of cytokine secretion from primary target cells. A direct dSLIM-dependent modulation was observed with TLR-9-positive cells, pDCs and B cells, with respect to costimulatory cell surface markers (CD80, CD86, CD40 (only B cells), and OX-40 (only on pDCs), downregulation of the inhibitory DCIR (only on pDCs)), and elevated cytokine secretion (MIP-1α, MIP-1β, IL-6, TNF-α, and IL-8 from both cell types; elevated secretion of IFN-α from pDCs exclusively). Additionally, TLR-9-negative cells such as T, NK, NKT cells, mDCs, and monocytes were activated upon exposure to dSLIM. These should be considered as indirect

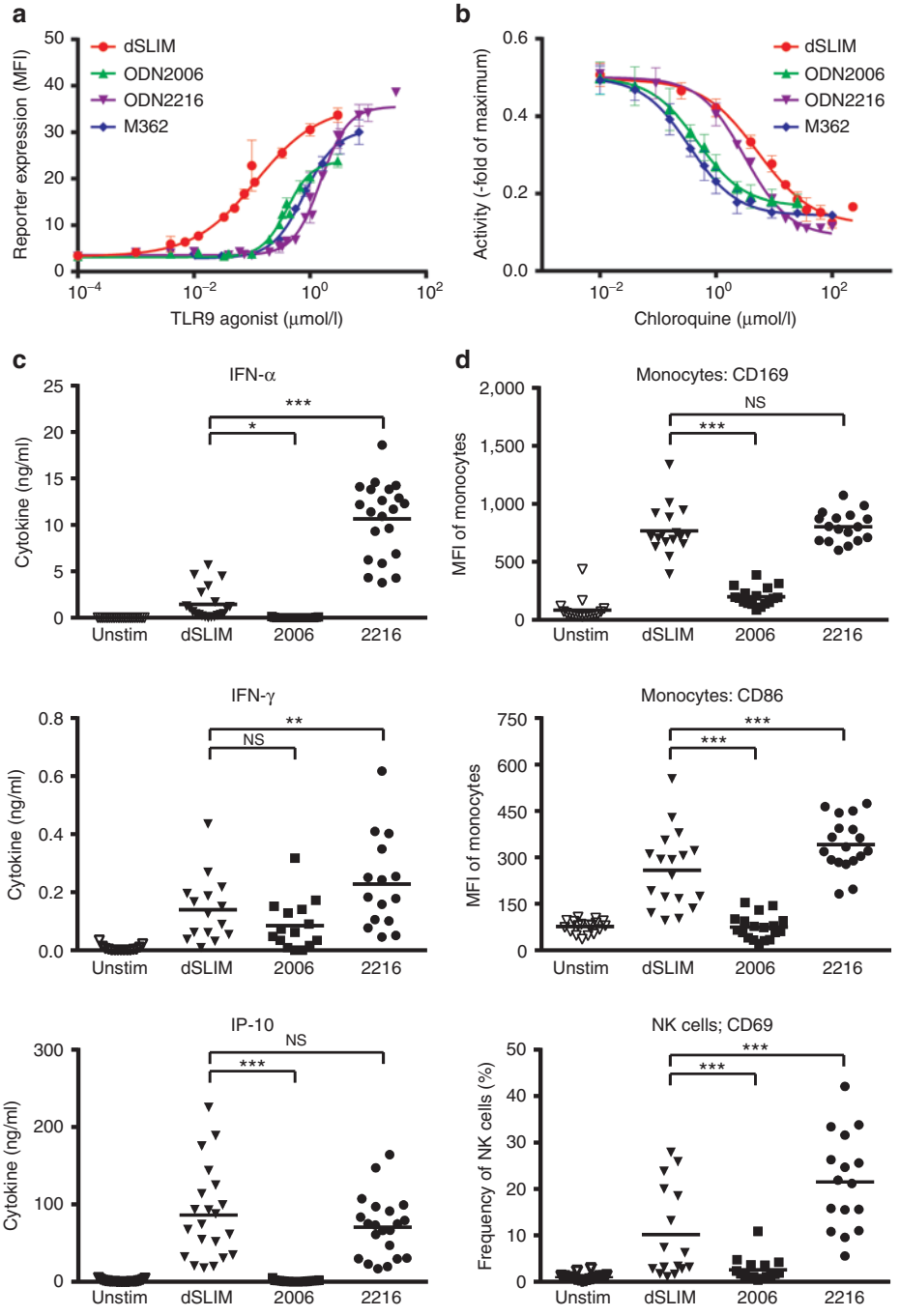

Figure 7 Immunomodulatory effects of double-Stem Loop ImmunoModulator (dSLIM) and CpG ODNs. (**a**) ELAM41 cells were stimulated with increasing concentrations of CpG ODN or dSLIM. dSLIM (red circle, $n = 13$; Hill slope 0.8; EC_{50} 0.1 µmol/l), class A (ODN2216, purple triangle up, $n = 10$; Hill slope 1.9; EC_{50} 1.4 µm), class B (ODN2006, green triangle down, $n = 10$; Hill slope 2; EC_{50} 0.4 µmol/l), class C (M362, blue diamond, $n = 5$, Hill slope 1.6; EC_{50} 0.8 µmol/l). The means of mean fluorescent intensity and SEM for the indicated number of individual experiments are shown. (**b**) ELAM41 cells were half maximally stimulated with dSLIM (0.1 µmol/l), ODN2216 (1.4 µmol/l), ODN2006 (0.4 µmol/l), or M362 (0.8 µmol/l) in the presence of increasing concentrations of the TLR-9 signaling inhibitor chloroquine. For each individual experiment, the mean fluorescence of living ELAM41 cells was normalized to the fluorescence analyzed after incubation with saturating agonist concentrations of 10 µmol/l. (**c,d**) PBMCs were incubated with dSLIM, ODN2216, or ODN2006 at a final concentration of 3 µmol/l for 48 hours. (**c**) Secreted cytokines. Cytokine levels in the supernatants were determined by a bead-based multiplex immunoassay or enzyme-linked immunosorbent assay (means are shown; IFN-α and IP-10, $n = 21$, each; IFN-γ, $n = 15$, only differences between dSLIM and the two CpG ODN were evaluated; $^{*}P < 0.05$; $^{**}P < 0.01$; $^{***}P < 0.001$; repeated measures analysis of variance (ANOVA); Fisher's least significant difference (LSD) test). (**d**) Cellular activation. Peripheral blood mononuclear cells were stained with antibodies against lineage and the indicated activation markers. Frequencies or geometric means of activation markers within the cell populations are shown (means are shown; CD86 of monocytes, $n = 18$, CD169 of monocytes, $n = 17$, CD69 of NK cells, $n = 16$, only differences between dSLIM and the two CpG ODN were evaluated; $^{*}P < 0.05$; $^{**}P < 0.01$; $^{***}P < 0.001$; repeated measures ANOVA; Fisher's LSD test).

effects of dSLIM, as no NK cell, monocyte, or mDC activation could be observed after removal of pDCs from the PBMC suspension. The most relevant cytokines responsible for this indirect effect of dSLIM on TLR-9-negative cells were (i) IFN-α, exclusively released from pDCs, and (ii) MIP-1α, MIP-1β, IL-6, TNF-α, and IL-8 released from pDCs, as well as B cells.

Exposure to dSLIM released IFN-α from pDCs and upregulated CD169 in monocytes from PBMCs; the expression of CD169 has recently been shown to be part of a type I IFN response.[25,26] The emerging picture suggests a dSLIM triggered activation cascade, in which dSLIM directly activates pDCs by TLR-9 stimulation to secrete IFN-α, which results in this strong activation of an immune response also involving TLR-9-negative immunomodulatory cells. IFN-γ and IP-10 secretions were upregulated after activation of PBMCs with dSLIM, but not from isolated pDCs or B cells. Furthermore, IFN-γ and IP-10 secretion from PBMCs continued after B cell removal, indicating that the source of these cytokines was from a different cell type within the PBMC pool. IFN-γ has to be ascribed to NK and NKT cell secretion while monocytes were shown to be the main source for the chemokine IP-10.

All observed effects of dSLIM were abolished after pDC removal, and considerably diminished after B cell removal from PBMCs, implying that TLR-9-positive cells play a major role in the mechanism of action of dSLIM. TLR-9 is known to be stimulated by unmethylated CpG of DNA molecules. When all CG motifs in dSLIM loops were switched to TpGs, the non-CG dSLIM no longer activated immune cells (see **Figure 3c**; **Supplementary Figures S3 and S4**) or the reconstructed signaling cascade in ELAM41 cells (see **Figure 6a**). We cannot exclude that after forced delivery via transfection into early endosomes, non-CG dSLIM may exert some TLR-9 activation similar to that shown by Haas *et al.*[27] for phosphodiester oligonucleotides. However, genuine uptake of non-CG dSLIM resulted in cellular activity and cytokine secretion not significantly different from activities of unstimulated cells, and thereby followed CpG-specificities shown for class A TLR-9 agonists.[16,28] Similar to other TLR-9 agonists, dSLIM activation was impeded by inhibitory[29] DNA ODNs (data not shown) or chloroquine.

dSLIM exhibits a unique structure that results in an individual biologic signature: dSLIM has six CpGs per molecule, with three clustered in each loop. At temperatures up to 37 °C, at least one CpG in each loop is predicted to be unpaired and free for TLR-9 binding; up to ≈53 °C intraloop base pairing becomes less probable, exposing up to three CpGs in each loop, while the double-stranded stem is minimally molten under 80 °C. Consequently, dSLIM provides a two-ligand scaffold for TLR-9 dimerization that may be reflected by the Hill slope of 0.8 developed for ELAM41 cells. In contrast, class A (ODN2216, Hill Slope 1.9) and class C (M362, Hill Slope 1.6) CpG ODNs may form higher order structures to stimulate TLR-9. The required aggregation of CpG ODNs before TLR-9 activation may also result in the higher EC_{50} values displayed by members of class A and C TLR-9 agonists compared to dSLIM. Those high molecular weight structures have been proposed to be necessary for specific endosomal translocation[30,31] and obviously were matched by dSLIM's proprietary defined structure. On the other hand, cellular uptake by mouse macrophages was indistinguishable from ODN2006 uptake (5 minutes time resolution; data not shown).

The structure of dSLIM results in a unique biologic footprint where dSLIM displays an immunomodulatory profile, which is distinct in quality and quantity from that of all three CpG ODN classes. With good activation of pDCs and moderate activation of B cells, dSLIM-mediated cellular activation differs from ODN2006 effects. The low efficiency of ODN2006 seen on ELAM41 cells may be attributed to toxic effects of the many phosphorothioates present in its backbone. Similarly, ODN2006 stimulatory effect on cytokine secretion from PBMC was limited to very low doses (see **Supplementary Figure S6**). Of the three classical ODN types of TLR-9 agonists studied, ODN2216 was the most similar to dSLIM in terms of activating pDCs, B cells, monocytes, and NK cells, and releasing IP-10 and IFN-γ, although it was associated with significantly more IFN-α production. It remains to be seen if such a tremendous IFN-α release results in a superior overall immunologic response against infections or cancer cells: although ODN2216 induced almost a 10-fold higher IFN-α secretion from pDCs than dSLIM, the second line of activation, *i.e.*, monocyte activation, was equally pronounced with ODN2216 or dSLIM.

Direct and indirect actions of dSLIM resulted in strong activation of the key players of the innate immune response: monocytes (which secrete immunomodulatory cytokines and remove antigens from blood and lymph by internalization), and NK cells (responsible for secreting additional immunomodulatory cytokines and selectively eliminating harmed cells by inducing apoptosis). This specific cytotoxic effect of NK cells against tumor cells was shown to be induced by dSLIM. Activation of dendritic cells as antigen-presenting cells, activation of T cells, and activation of B cells take place simultaneously, synergizing with the regulated IFN-γ secretion to induce the T_H1 arm of the adaptive immune response. The adaptive arm of antitumor response is further enforced by type I IFN activating CD8-α-positive dendritic cells that cross-present antigens to cytotoxic T cells.[32–34] Furthermore, dSLIM-activated monocytes differentiate into CD169-bearing macrophages that have been shown to be involved in the cross-presentation of tumor-associated antigens in mice.[35,36] Such strong activation of both innate and adaptive immune response is thought to be a prerequisite for an effective antitumor response,[37] further enhanced by dSLIM activation of monocytes to release the angiostatic[38,39] IP-10.

All effects of dSLIM described here at the molecular and cellular level translate well into systemic effects: In mouse studies, tumor cell vaccination utilizing a syngeneic system was shown to be enhanced by dSLIM,[40] affirming *in vivo* the broad immunomodulatory effect of dSLIM observed *in vitro* on key cells of both the innate as well as adaptive immune response. dSLIM is also being tested in humans as an adjuvant in a cell-based therapeutic vaccine against tumor-associated antigens. In this clinical study (ASET, registered #NCT01265368), dSLIM combined with gene-modified, allogeneic tumor cells (MGN1601) shows promising preliminary efficacy in patients with late stage metastatic renal cell carcinoma disease.[41]

dSLIM molecules (MGN1703) are under investigation in a phase 2 clinical trial metastatic colorectal carcinoma (IMPACT, registered #NCT01208194).[42] In this study where bi-weekly 60 mg of MGN1703 was subcutaneously applied,

dSLIM was well tolerated with some patients have been receiving treatment in excess of 2 years without major adverse effects.[43] One important reason for such a smooth transition from basic research into clinical efficacy may be the sustained concentration–efficacy relation illustrated on model ELAM41 cells as well as isolated PBMCs and cellular subpopulations thereof. Furthermore, dSLIM did not show inhibitory effects on its primary targets pDCs and B cells even at concentrations 10-fold higher than routinely used for immunoactivation. The lack of detectable systemic toxicity of dSLIM may be due its composition of only natural, *i.e.*, nonmodified DNA, granting the mere absence of TLR-9 off-target effects. Clinically, dSLIM maintenance treatment improves progression-free survival and shows durable disease control compared to placebo in patients with advanced colorectal cancer. In this IMPACT study, upregulation of CD169 on human circulating monocytes as part of the IFN-α signature was observed,[43] and we have also indication for activation of circulating pDCs.[44] Therefore, primary signaling cascades and subsequent pathways triggered by dSLIM on isolated PBMCs and model cell systems are also upregulated after systemic administration of dSLIM indicating that the presented experimental data set of the immunomodulator dSLIM finds confirmation *in vivo*.

Materials and methods

Immunomodulatory DNA molecules. dSLIM was generated from eODN CTAGGGGTTACCACCTTCATTGGAAAA *CG*TTCTT *CG*GGG *CG*TTCTTAGGTGGTAACCC by dimer-circularization according to Schmidt *et al.*[45] Non-CG dSLIM was synthesized from ODN CTAGGGGTTACCACCTTCATTGG AAAA *TG*TTCTT *TG*GGG *TG*TTCTTAGGTGGTAACCC. CpG ODNs ODN2216, ODN2006, and M362 were synthesized by Microsynth (Balgach, Switzerland) or TIB Molbiol (Berlin, Germany).

The conformational structure of dSLIM under isotonic conditions was calculated using the mfold web server http://www.bioinfo.rpi.edu/applications/mfold/.[46]

Cell isolation and activation. Buffy coats from healthy donors were obtained from the "DRK-Blutspendedienst—Ost" (Berlin, Germany). PBMCs were isolated by density gradient centrifugation using Ficoll (Biochrom, Berlin, Germany; now Merck Millipore). pDCs were prepared using the Human Diamond pDC Isolation Kit (Miltenyi Biotec, Bergisch Gladbach, Germany) according to the manufacturer's instructions. pDCs were removed from PBMCs using the CD304 MicroBead Kit (Miltenyi Biotec). B cells were removed from PBMCs using the CD19 MicroBead Kit (Miltenyi Biotec).

Cells were cultured in complete medium (RPMI1640; Lonza, Basel, Switzerland) with 2 mmol/l UltraGlutamine (Lonza) supplemented with 10% (v/v) fetal calf serum (Linaris, Dossenheim, Germany), 100 U/ml penicillin, and 100 µg/ml streptomycin in flat-bottom plates (6 million PBMCs/ml, 2 million B cells/ml) or 96-well round bottom plates (0.25 million pDCs/ml, in the presence of 10 ng/ml recombinant IL-3 (PeproTech, Hamburg, Germany)).

Cytotoxicity assay. Jurkat cells (DSMZ, Braunschweig, Germany) were used as target cells and labeled for 5 minutes at 37 °C in RPMI1640 (Lonza) with the lipophilic dye DiI (Invitrogen/Life Technologies, Darmstadt, Germany) at a final concentration of 1 µmol/l. After 18 hours, 50,000 target cells were cocultured with effector cells (treated PBMCs) in three different ratios (effector: target 20:1, 10:1, and 5:1). For positive control, PBMCs were cultured in 2,000 U/ml IL-2 (PeproTech). Cultures were performed in complete medium and were run for 4 hours at 37 °C in 96-well round bottom plates in duplicates. Subsequently, cells were stained with 7-AAD (BD Biosciences, Heidelberg, Germany). On a FACSCalibur (BD Biosciences), 5,000 target cells were acquired. The percentage of dead target cells was determined from 7-AAD-positive cells and specific cytotoxicity was calculated:

$$\text{Specific cytotoxicity (\%)} = ((\text{\% 7-AAD}^+ \text{ of DiI}^+_{\text{induced}}) - (\text{\% 7-AAD}^+ \text{ of DiI}^+_{\text{spontaneous}}))/(100 - \text{\% 7-AAD}^+ \text{ of DiI}^+_{\text{spontaneous}})*100.$$

NFκB reporter assay and flow cytometry. Mouse macrophages RAW 264.7 cells were transfected with the *cds* of d2-eGFP (Takara Bio Europe/Clontech, Saint-Germain-en-Laye, France) under an optimized promoter of the human elastin gene (Entrez Gene ID 2006). The promoter region had been amplified from genomic DNA using primers CKm512fw TCGCGAGCCACTGTGCCTGGCCTCC (*Bsp*68I) and CKm513rev GGTCTCAGGCGGCCTGCTGCC TCTGTTTCAGGTC (*Eco*31I), and ligated to appropriately generated termini of the cDNA of d2-eGFP (*Eco*31I/*Eco*RI) into pcDNA3.1(-)(*Bsp*68I/*Eco*RI; Invitrogen). Stable transfected cells were selected for G418 resistance to generate the stable cell line ELAM41. ELAM41 cells were seeded at a density of 125,000/cm^2. After 24 hours at 37 °C, immunomodulatory DNA was added for another 7 hours at the indicated concentrations.

All flow cytometric parameters of cells were acquired on a FACSCalibur. Frequencies were related to living cells, or parent populations were indicated; geometric means of fluorescent cells were indicated as mean fluorescent intensity. Data were analyzed with the FlowJo software (Tree Star, Ashland, Oregon).

Cell surface staining for activation. Extracellular plasma membrane-bound proteins were stained on intact cells with monoclonal antibodies in phosphate-buffered saline containing 10% (v/v) human serum, 2.5% (v/v) fetal calf serum, and 0.1% (w/v) azide on ice. The following antibodies were used: anti-lineage cocktail 1, anti-CD123 (7G3), anti-HLA-DR (L243), anti-CD40 (5C3), anti-CD11c (B-ly6), anti-CD86 (2331 FUN-1), anti-CD19 (4G7), anti-CD69 (FN50), all from BD Biosciences; anti-CD14 (61D3), anti-CD169 (7–239), anti-CD3 (OKT-3), anti-CD56 (MEM188), anti-CD80 (2D10), all from eBioscience (Frankfurt a.M, Germany).

Determination of cytokines. Secreted cytokines were accumulated in cell growth medium for 2 days if not indicated otherwise. Enzyme-linked immunosorbent assays for IFN-α (eBioscience), IFN-γ (OptEIA Human IFN-γ ELISA Set, BD Biosciences), IP-10, IL-8, and MCP-1 (all from R&D Systems,

Wiesbaden-Nordenstadt, Germany) were performed in duplicates according to the manufacturer's instructions. Optical density was measured at 450 nm; the data were analyzed with the MicroWin software (Berthold Technologies, Bad Wilbad, Germany).

Alternatively, cytokine levels in the cell growth medium were determined in duplicates by a bead-based multiplex immunoassay (FlowCytomix from eBioscience) according to the manufacturer's instructions. Data were acquired on a FACSCalibur and evaluated with the FlowCytomixPro software (eBioscience).

Statistical analysis. Data were analyzed with GraphPad Prism 6 (GraphPad Software, La Jolla, CA). If not otherwise indicated, means of the stated number of independent experiments are shown. The paired *t*-test was used to analyze differences between two culture conditions. Repeated measures one-way analysis of variance with Fisher's least significant difference test was used for the comparisons of three and more culture conditions and with Dunnett's multiple comparison test to compare the differences between activators and the negative control. $P < 0.05$ was considered significant.

Supplementary material

Figure S1. Thermal Dissociation of dSLIM and educt ODN.
Figure S2. Stability against exonuclease activity.
Figure S3. Cellular activation by non-CG dSLIM.
Figure S4. Cytokine secretion by non-CG dSLIM.
Figure S5. Monocytes are the IP-10 secreting cell population in PBMCs.
Figure S6. ODN2006 shows some activity at low concentrations.
Supplementary Data.

Acknowledgments. The authors thank Jacqueline Schneider, Lisa Schneider, Nadine Gollinge, Stefanie Jänsch (all Mologen AG), and Tomislav Dorbic (Freie Universitaet) for their excellent technical assistance. K.K., C.K., and M.S. are employees of Mologen AG, B.W. consulted Mologen AG and also received funding from Mologen AG; all authors have commercial interest in the therapeutic development of dSLIM, but have no additional financial interests.

1. Kawai, T and Akira, S (2010). The role of pattern-recognition receptors in innate immunity: update on Toll-like receptors. *Nat Immunol* **11**: 373–384.
2. Hemmi, H, Takeuchi, O, Kawai, T, Kaisho, T, Sato, S, Sanjo, H *et al.* (2000). A Toll-like receptor recognizes bacterial DNA. *Nature* **408**: 740–745.
3. Oka, T, Hikoso, S, Yamaguchi, O, Taneike, M, Takeda, T, Tamai, T *et al.* (2012). Mitochondrial DNA that escapes from autophagy causes inflammation and heart failure. *Nature* **485**: 251–255.
4. Zhang, Q, Raoof, M, Chen, Y, Sumi, Y, Sursal, T, Junger, W *et al.* (2010). Circulating mitochondrial DAMPs cause inflammatory responses to injury. *Nature* **464**: 104–107.
5. Hornung, V, Rothenfusser, S, Britsch, S, Krug, A, Jahrsdörfer, B, Giese, T *et al.* (2002). Quantitative expression of toll-like receptor 1-10 mRNA in cellular subsets of human peripheral blood mononuclear cells and sensitivity to CpG oligodeoxynucleotides. *J Immunol* **168**: 4531–4537.
6. Iwasaki, A and Medzhitov, R (2004). Toll-like receptor control of the adaptive immune responses. *Nat Immunol* **5**: 987–995.
7. Guiducci, C, Coffman, RL and Barrat, FJ (2009). Signalling pathways leading to IFN-alpha production in human plasmacytoid dendritic cell and the possible use of agonists or antagonists of TLR7 and TLR9 in clinical indications. *J Intern Med* **265**: 43–57.
8. Kawai, T and Akira, S (2007). TLR signaling. *Semin Immunol* **19**: 24–32.
9. Ito, T, Kanzler, H, Duramad, O, Cao, W and Liu, YJ (2006). Specialization, kinetics, and repertoire of type 1 interferon responses by human plasmacytoid predendritic cells. *Blood* **107**: 2423–2431.
10. Colonna, M, Trinchieri, G and Liu, YJ (2004). Plasmacytoid dendritic cells in immunity. *Nat Immunol* **5**: 1219–1226.
11. Zhang, Z and Wang, FS (2005). Plasmacytoid dendritic cells act as the most competent cell type in linking antiviral innate and adaptive immune responses. *Cell Mol Immunol* **2**: 411–417.
12. Poeck, H, Wagner, M, Battiany, J, Rothenfusser, S, Wellisch, D, Hornung, V *et al.* (2004). Plasmacytoid dendritic cells, antigen, and CpG-C license human B cells for plasma cell differentiation and immunoglobulin production in the absence of T-cell help. *Blood* **103**: 3058–3064.
13. Klinman, DM (2004). Immunotherapeutic uses of CpG oligodeoxynucleotides. *Nat Rev Immunol* **4**: 249–258.
14. Krieg, AM (2007). Development of TLR9 agonists for cancer therapy. *J Clin Invest* **117**: 1184–1194.
15. Vollmer, J and Krieg, AM (2009). Immunotherapeutic applications of CpG oligodeoxynucleotide TLR9 agonists. *Adv Drug Deliv Rev* **61**: 195–204.
16. Krug, A, Rothenfusser, S, Hornung, V, Jahrsdörfer, B, Blackwell, S, Ballas, ZK *et al.* (2001). Identification of CpG oligonucleotide sequences with high induction of IFN-alpha/beta in plasmacytoid dendritic cells. *Eur J Immunol* **31**: 2154–2163.
17. Verthelyi, D, Ishii, KJ, Gursel, M, Takeshita, F and Klinman, DM (2001). Human peripheral blood cells differentially recognize and respond to two distinct CPG motifs. *J Immunol* **166**: 2372–2377.
18. Hartmann, G and Krieg, AM (2000). Mechanism and function of a newly identified CpG DNA motif in human primary B cells. *J Immunol* **164**: 944–953.
19. Hartmann, G, Battiany, J, Poeck, H, Wagner, M, Kerkmann, M, Lubenow, N *et al.* (2003). Rational design of new CpG oligonucleotides that combine B cell activation with high IFN-alpha induction in plasmacytoid dendritic cells. *Eur J Immunol* **33**: 1633–1641.
20. Marshall, JD (2003). Identification of a novel CpG DNA class and motif that optimally stimulate B cell and plasmacytoid dendritic cell functions. *J Leukoc Biol* **73**: 781–792.
21. Sato, Y, Roman, M, Tighe, H, Lee, D, Corr, M, Nguyen, MD *et al.* (1996). Immunostimulatory DNA sequences necessary for effective intradermal gene immunization. *Science* **273**: 352–354.
22. Heikenwalder, M, Polymenidou, M, Junt, T, Sigurdson, C, Wagner, H, Akira, S *et al.* (2004). Lymphoid follicle destruction and immunosuppression after repeated CpG oligodeoxynucleotide administration. *Nat Med* **10**: 187–192.
23. Hirsh, V, Paz-Ares, L, Boyer, M, Rosell, R, Middleton, G, Eberhardt, WE *et al.* (2011). Randomized phase III trial of paclitaxel/carboplatin with or without PF-3512676 (Toll-like receptor 9 agonist) as first-line treatment for advanced non-small-cell lung cancer. *J Clin Oncol* **29**: 2667–2674.
24. Steinman, RM, Mellman, IS, Muller, WA and Cohn, ZA (1983). Endocytosis and the recycling of plasma membrane. *J Cell Biol* **96**: 1–27.
25. Biesen, R, Demir, C, Barkhudarova, F, Grün, JR, Steinbrich-Zöllner, M, Backhaus, M *et al.* (2008). Sialic acid-binding Ig-like lectin 1 expression in inflammatory and resident monocytes is a potential biomarker for monitoring disease activity and success of therapy in systemic lupus erythematosus. *Arthritis Rheum* **58**: 1136–1145.
26. York, MR, Nagai, T, Mangini, AJ, Lemaire, R, van Seventer, JM and Lafyatis, R (2007). A macrophage marker, Siglec-1, is increased on circulating monocytes in patients with systemic sclerosis and induced by type I interferons and toll-like receptor agonists. *Arthritis Rheum* **56**: 1010–1020.
27. Haas, T, Metzger, J, Schmitz, F, Heit, A, Müller, T, Latz, E *et al.* (2008). The DNA sugar backbone 2' deoxyribose determines toll-like receptor 9 activation. *Immunity* **28**: 315–323.
28. Vollmer, J, Weeratna, R, Payette, P, Jurk, M, Schetter, C, Laucht, M *et al.* (2004). Characterization of three CpG oligodeoxynucleotide classes with distinct immunostimulatory activities. *Eur J Immunol* **34**: 251–262.
29. Duramad, O, Fearon, KL, Chang, B, Chan, JH, Gregorio, J, Coffman, RL *et al.* (2005). Inhibitors of TLR-9 act on multiple cell subsets in mouse and man *in vitro* and prevent death *in vivo* from systemic inflammation. *J Immunol* **174**: 5193–5200.
30. Guiducci, C, Ott, G, Chan, JH, Damon, E, Calacsan, C, Matray, T *et al.* (2006). Properties regulating the nature of the plasmacytoid dendritic cell response to Toll-like receptor 9 activation. *J Exp Med* **203**: 1999–2008.
31. Honda, K, Ohba, Y, Yanai, H, Negishi, H, Mizutani, T, Takaoka, A *et al.* (2005). Spatiotemporal regulation of MyD88-IRF-7 signalling for robust type-I interferon induction. *Nature* **434**: 1035–1040.
32. Diamond, MS, Kinder, M, Matsushita, H, Mashayekhi, M, Dunn, GP, Archambault, JM *et al.* (2011). Type I interferon is selectively required by dendritic cells for immune rejection of tumors. *J Exp Med* **208**: 1989–2003.
33. Fuertes, MB, Kacha, AK, Kline, J, Woo, SR, Kranz, DM, Murphy, KM *et al.* (2011). Host type I IFN signals are required for antitumor CD8+ T cell responses through CD8{alpha}+ dendritic cells. *J Exp Med* **208**: 2005–2016.
34. Fuertes, MB, Woo, SR, Burnett, B, Fu, YX and Gajewski, TF (2013). Type I interferon response and innate immune sensing of cancer. *Trends Immunol* **34**: 67–73.
35. Asano, K, Nabeyama, A, Miyake, Y, Qiu, CH, Kurita, A, Tomura, M *et al.* (2011). CD169-positive macrophages dominate antitumor immunity by crosspresenting dead cell-associated antigens. *Immunity* **34**: 85–95.

36. Martinez-Pomares, L and Gordon, S (2012). CD169+ macrophages at the crossroads of antigen presentation. *Trends Immunol* **33**: 66–70.
37. Vesely, MD, Kershaw, MH, Schreiber, RD and Smyth, MJ (2011). Natural innate and adaptive immunity to cancer. *Annu Rev Immunol* **29**: 235–271.
38. Arenberg, DA, Kunkel, SL, Polverini, PJ, Morris, SB, Burdick, MD, Glass, MC *et al.* (1996). Interferon-gamma-inducible protein 10 (IP-10) is an angiostatic factor that inhibits human non-small cell lung cancer (NSCLC) tumorigenesis and spontaneous metastases. *J Exp Med* **184**: 981–992.
39. Belperio, JA, Keane, MP, Arenberg, DA, Addison, CL, Ehlert, JE, Burdick, MD *et al.* (2000). CXC chemokines in angiogenesis. *J Leukoc Biol* **68**: 1–8.
40. Volz, B, Schmidt, M, Kapp, K, Schroff, M, Tschaika, M and Wittig, B. Presented at: 13th Annual Meeting of the American Society of Gene and Cell Therapy, Washington DC, USA, 19–22 May 2010, *Mol Ther* **18**: abstract 822.
41. Grünwald, V, Weikert, S, Schmidt-Wolf, IGH, Hauser, S, Weith, E, Schroff, M, *et al.* Presented at: 2013 Annual Meeting of the American Society of Clinical Oncology in Rosen Shingle Creek, Orlando, FL, USA, 14–16 February 2013. *J Clin Oncol* **31**: abstract 468.
42. Tschaika, M, Schmoll, HJ, Riera-Knorrenschild, J, Nitsche, D, Trojan, J, Kröning, H, *et al.* Presented at: 2012 Annual Meeting of the American Society of Clinical Oncology, San Francisco CA, USA, 19–21 January 2012. *J Clin Oncol* **30**: abstract 633.
43. Schmoll, HJ, Riera-Knorrenschild, J, Kroening, H, Mayer, F, Nitsche, D, Ziebermayr, R, *et al.* Presented at: 2013 Annual Meeting of the European Society of Medical Oncology, Barcelona, Spain, 3–6 July 2013. *Ann Oncol* **24**: abstract O-0012.
44. Schmoll, HJ, Witting, B, Arnold, D, Riera-Knorrenschild, J, Nitsche, D, Kroening, H, *et al.* (2014). Maintenance treatment with the immunomodulator MGN1703, a Toll-like receptor 9 (TLR9) agonist, in patients with metastatic colorectal carcinoma and disease control after chemotherapy: a randomised , double-blind, placebo-controlled trial. *J Cancer Res Clin Oncol* (epub ahead of print).
45. Schmidt, M, Anton, K, Nordhaus, C, Junghans, C, Wittig, B and Worm, M (2006). Cytokine and Ig-production by CG-containing sequences with phosphorodiester backbone and dumbbell-shape. *Allergy* **61**: 56–63.
46. Zuker, M (2003). Mfold web server for nucleic acid folding and hybridization prediction. *Nucleic Acids Res* **31**: 3406–3415.

Supplementary Information accompanies this paper on the Molecular Therapy–Nucleic Acids website (http://www.nature.com/mtna)